Journal of Sound and Vibration 329 (2010) 2477–2489

Contents lists available at ScienceDirect

Journal of Sound and Vibration

journal homepage: www.elsevier.com/locate/jsvi

Broadband flow-induced sound control using plasma actuators

Xun Huang [a,b,*], Xin Zhang [b], Yong Li [b]

[a] State Key Laboratory of Turbulence and Complex Systems, Department of Mechanical and Aerospace Engineering, College of Engineering, Peking University, China

[b] Aeronautics and Astronautics, School of Engineering Sciences, University of Southampton, UK

ARTICLE INFO

Article history:
Received 15 April 2009
Received in revised form
3 January 2010
Accepted 15 January 2010
Handling Editor: L.G. Tham
Available online 9 February 2010

ABSTRACT

Plasma actuators were used in this work to control flow-induced broadband noise radiated from a bluff body. The model consists of a cylinder and a component (torque link) that is installed on the lee side of the cylinder. The objective is to reduce the broadband noise mainly generated through the impingement of the cylinder wake on the torque link. The flow–structure interactions between the cylinder wake and the torque link are reduced by manipulating the cylinder wake with the externally imposed body force from the plasma actuators, which lead to the attenuation of the broadband noise. The control performance with the plasma actuators is studied in an anechoic chamber facility by examining far-field sound level and near-field acoustic source changes. At a free stream speed of 30 m/s, corresponding to the Reynolds number of 2.1×10^5, far-field measurements suggested that a reduction of up to 3.2 dB in overall sound pressure level. The near-field beamforming results also show approximately 3 dB reduction in the interested frequency ranges. The physical mechanisms related to broadband noise control were also discussed. This work suggests that plasma actuators offer the potential for solving flow-induced noise control problem at broadband frequencies.

1. Introduction

Plasma actuators [1] hold the potential to reduce flow-induced noise from airframe through modifying the adjacent flow field [2]. The simplicity and the absence of any mechanical moving parts make plasma actuators a promising option for flow/noise control applications. Recent work [3–6] has demonstrated the potential of plasma actuators [7,8] in the attenuation of tonal noise from a cavity. The more difficult problem of broadband noise control with plasma actuators is studied in this work.

Most latest flow control applications with plasma include: (1) high-speed flow control by localized arc filament plasma actuators [9], surface impulse discharges [10] and glow discharges [11]; (2) flat plate boundary layer flow control by non-thermal direct current (DC) corona discharge [12]; (3) airfoil separation control by glow discharge plasma actuators [1]; and (4) airfoil wake control by dielectric barrier discharge (DBD) plasma actuators [13]. A more complete review of the history and principle of plasma actuators can be found in the literature [14] and references therein. The plasma actuators of the DBD type are used throughout this work for a low-speed flow/noise control application. For brevity the name of the plasma actuators only applies to the DBD plasma actuators in the rest of the paper.

Through ionization the plasma actuators generate weakly ionized atmospheric plasma that consists of charged particles, which are moved within the coupled electric field [15]. Through collisions between the charged particles and the

* Corresponding author.
E-mail address: huangxun@pku.edu.cn (X. Huang).

0022-460X/$ - see front matter © 2010 Elsevier Ltd. All rights reserved.
doi:10.1016/j.jsv.2010.01.018

ambient particles, the plasma actuators act as a jet along the actuator surface. The maximal induced jet velocity is up to 8 m/s measured at 20 mm away from the electrodes [6].

For flow-induced noise control applications, the plasma actuators attenuated tonal noise from a cavity successfully through either manipulating shear layer [3] or generating disturbances at an off-resonant frequency [6]. The actuation bandwidth can be extended using a modulation technique [4]. A linear model was also presented for the plasma actuators from the perspective of control [5]. In this work, the interest was focused on a more difficult sound control problem: the attenuation of broadband noise generated from a bluff body.

Previous work has been performed on a single cylinder at Reynolds numbers between 1×10^4 and 4×10^4 [16–18]. It was found that the cylinder wake width can be controlled and vortex shedding from the cylinder could be suppressed. Specifically, it has been found that the downstream flow appeared to be fully attached under a downstream-directed plasma actuation [16,17]. On the other hand, the separation is promoted under an upstream-directed plasma actuation [17]. The definitions of the upstream- and the downstream-directed actuations are given in the following sections.

In the present work the attenuation of broadband noise generated by a more complex bluff body geometry, which represents a simplified landing gear component, is investigated using near- and far-field microphones. The control effectiveness of the upstream- and downstream-directed plasma actuations has been compared in this work. The paper is organized as follows. Section 2 introduces the fundamentals of the plasma actuator system used in this work. Section 3 gives the details of the experimental setup. Section 4 presents results and discussion. A summary of the present work is provided in Section 5.

2. Plasma actuators

Fig. 1 shows a typical plasma actuator system that includes a high voltage alternating current (AC) power supply and a plasma actuator [4]. Any arcing produced between electrodes can be prevented by the dielectric material. As a result, glow discharges with a uniform distribution of plasma can be produced. Rather than inserting strong heat waves to the adjacent flow, the plasma actuators control the flow using non-thermal mechanisms. Through ionization the plasma actuators generate weakly ionized atmospheric plasma that consists of charged particles, which are moved within the coupled

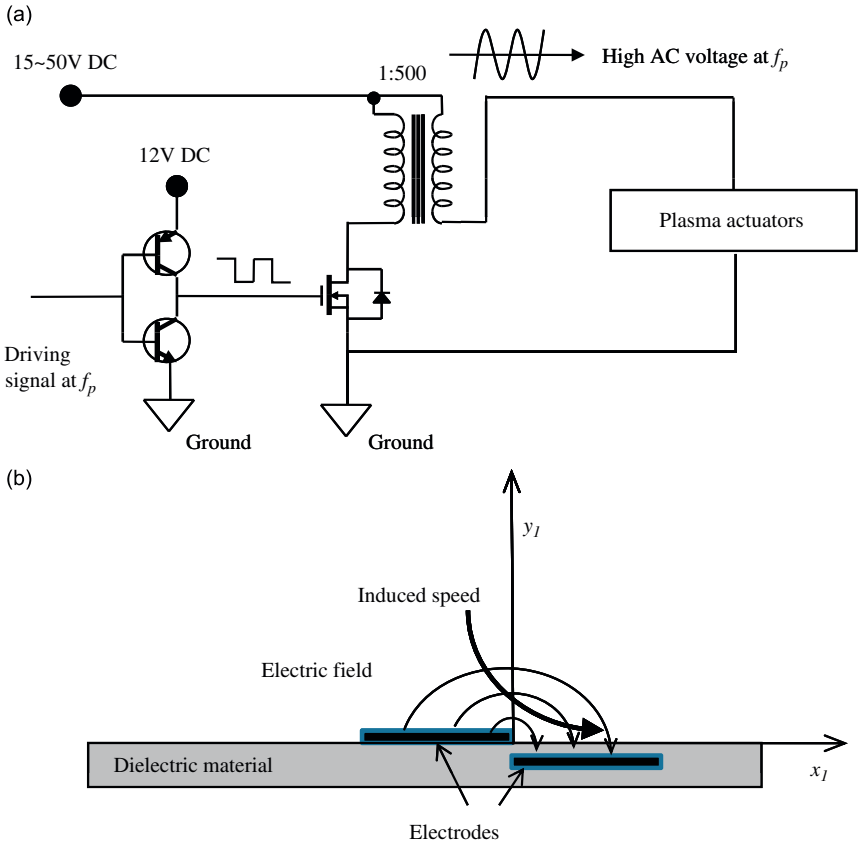

Fig. 1. Schematic of a plasma actuator system using (a) the topology of switching circuits, and (b) DBD plasma actuators.

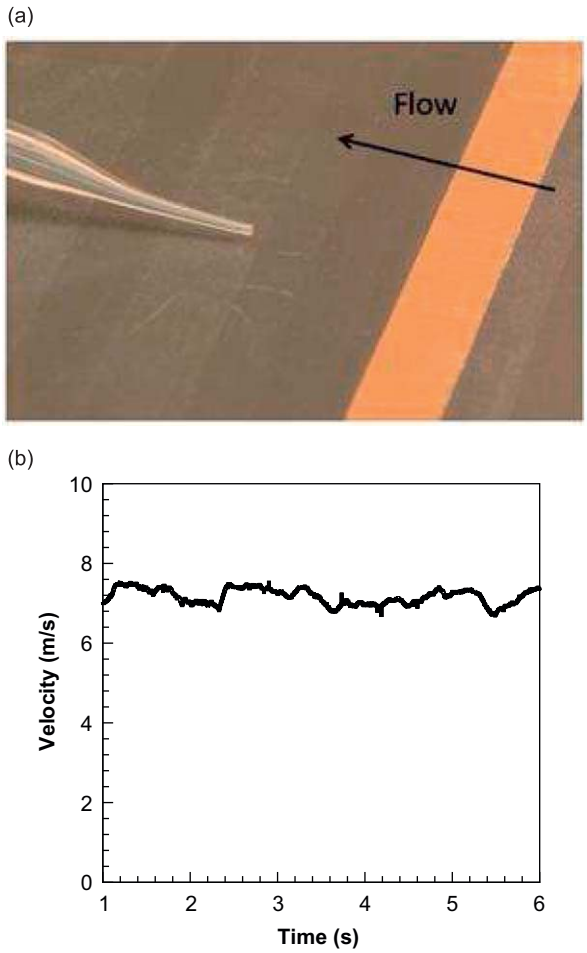

Fig. 2. Airflow velocity induced by plasma actuators, where (a) laboratory setup of velocity survey, and (b) induced velocity.

electric field. Through collisions between the charged particles and the ambient particles, the plasma actuators act as a jet along the actuator surface. The principle of using plasma actuators for aeroacoustic control is to sufficiently modify the flow field to disrupt or to alter the mechanisms of the generation of flow-induced noise.

As shown in Fig. 2, the maximal induced jet velocity is up to approximately 8 m/s measured at x_1 = 20 mm and y_1 = 1.5 mm. More detailed profiles at various testing positions can be found in our previous publications [19]. A high voltage signal of the sinusoid waveform at 3.5 kHz is applied to the plasma actuators. The frequency depends on the impedance of the plasma actuator. The peak-to-peak voltage V_{pp} = 25 kV. The thickness of the dielectric material (silicon rubber) is 2 mm. The width of the electrode exposed to air is 10 mm, while the insulated electrode is 20 mm. The power consumption in this experiment is approximately 5 W/mm. The dielectric constant of the dielectric material is 4.5 ± 0.5.

A sufficiently high electric field is required to break down the air species to generate atmospheric glow discharges. The power supply shown in Fig. 1 has a switching circuit topology that restricts the driving signal to a square wave and the output to a high voltage sinusoid wave. Specially, the driving signal switches a step up transformer through a power metal-oxide-semiconductor field-effect transistor (MOSFET). Two bipolar transistors form a push–pull gate driver to increase the driving ability and reduce the switching loss of the MOSFET devices. The high voltage output of a sinusoid waveform is applied to the DBD plasma actuators to sustain the discharges. Because a DBD plasma actuator can be regarded as a capacitive load, the whole DBD plasma system is an inductance–capacitance (LC) circuit from the electric viewpoint. The DBD plasma system should work most efficiently at the oscillation frequency (f_p) of the LC circuit. The driving frequency, f_p, could be increased beyond 20 kHz using a suitable impedance matching network [20] to reduce audible noise radiated from the plasma actuators. The switching-based power system shown in Fig. 1 is efficient in energy inversion but can only output a sinusoid wave. Up to now the sinusoid waveform is still used in many practical applications for its simplicity and efficiency.

3. Experimental apparatus

The geometry of the testing model is a $\frac{1}{4}$ scale representative of a landing gear strut, consisting of a cylinder and a component called torque link. The diameter of the cylinder is $D=100$ mm. The torque link is installed on the downstream side to the cylinder, formed by two triangle shaped plates at an angle $\alpha=90^{\circ}$ (see Fig. 3). The cylinder is made of a foam material to prevent electric interference from happening on plasma actuators. The torque link component is constructed from aluminum. A microphone (Panasonic WM-60A) is flush mounted to the surface of the torque link to record the surface pressure fluctuation. The sensitivity of the microphone is -45 ± 5 dBV/Pa. The diameter of the microphone is 6 mm and the thickness is 5 mm. A hole is drilled in the center of the toque link to contain the microphone (see Fig. 3). The diaphragm of the microphone faces the leading cylinder. Hence, the effect from the impingement of the cylinder wake flow on the torque link surface can be measured, which can be used to investigate the fluid–structure interaction. Only one

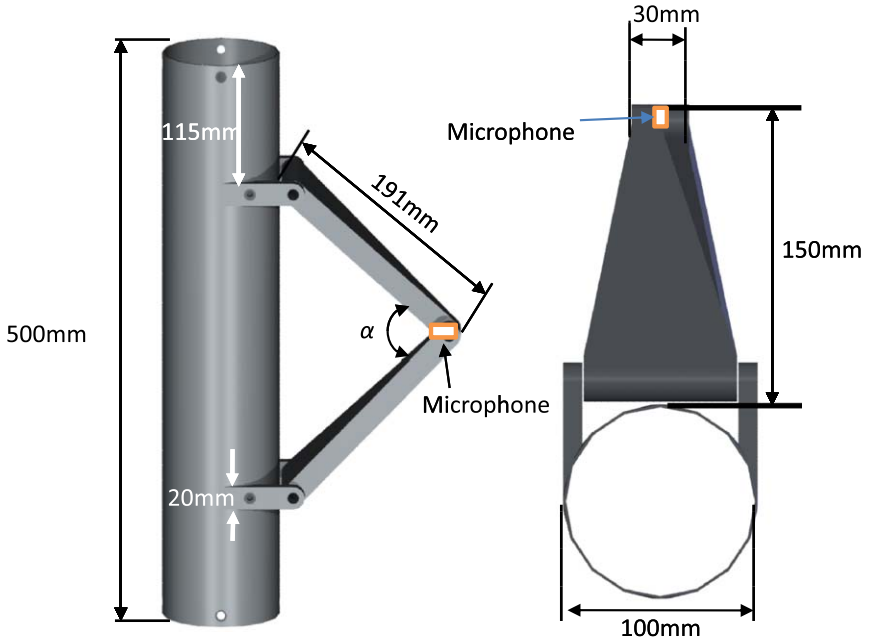

Fig. 3. Schematic of the testing model, (left) side view and (right) plan view.

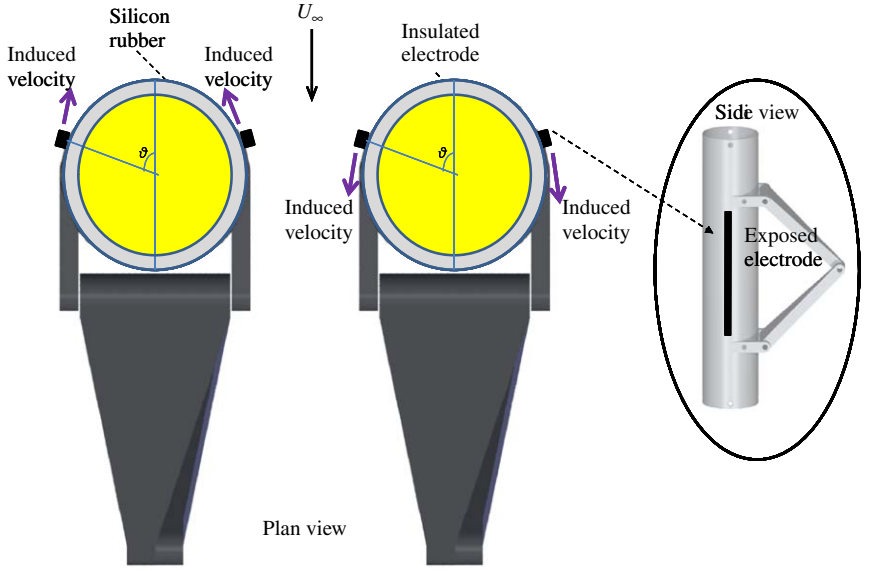

Fig. 4. Schematics of the testing model with plasma actuators.

microphone can be mounted on that position due to mechanical structure problem. The output from this microphone is passed through a hand-made anti-aliasing filter and is subsequently sampled at 20 kHz with a DS1104 system produced by dSPACE.

The noise radiating from the model is higher at broadband frequencies compared to that of the cases with a single cylinder model [16–18]. This increase is thought to be caused by the strong flow–structure interaction between the cylinder wake and the torque link. A couple of configurations of plasma actuators have been tested in this work to control the broadband noise.

Fig. 4 shows the layout of the plasma actuators installed on the surface of the cylinder. The thick black curves denote the electrodes made by copper tapes of thickness 0.04 mm. The width of the electrodes exposed to air is 10 mm. The width of the electrodes insulated by the dielectric material is 20 mm. The span length of the electrodes is 200 mm. The dielectric material is silicon rubber with a dielectric constant of 4.5 ± 0.5 and the thickness of 1 mm.

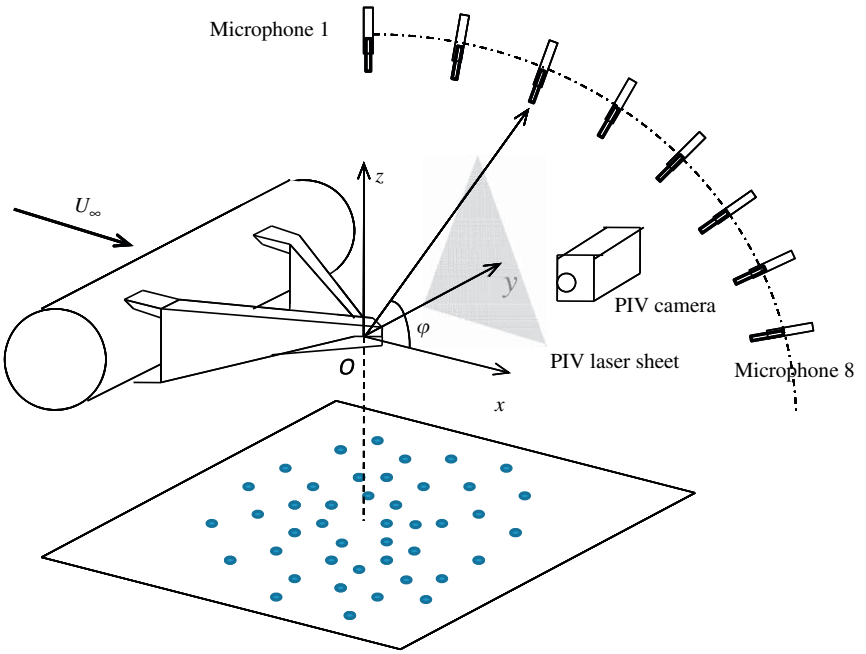

Fig. 5. Setup of the experiment units.

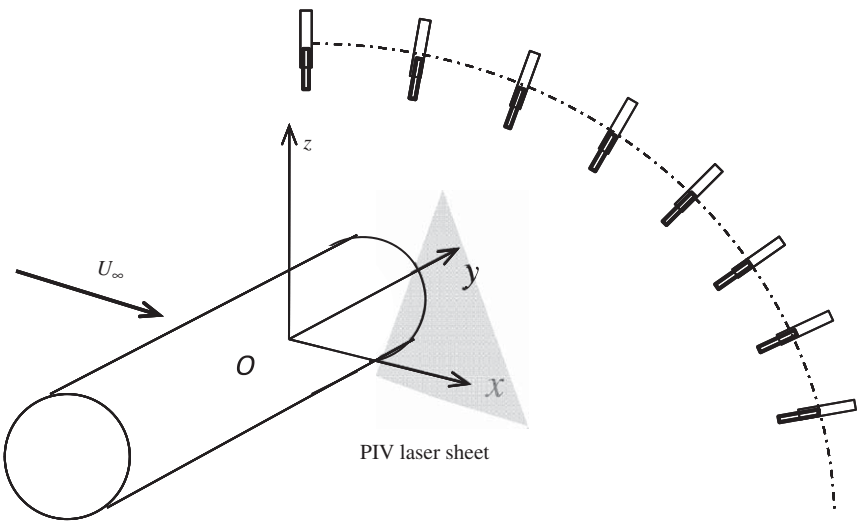

Fig. 6. The PIV setup for the single cylinder case.

The exposed electrodes in Fig. 4 are connected to the high voltage AC power supply. The insulated electrodes are grounded. To sustain the discharges, the AC voltage operates at a frequency on the order of kHz. The peak-to-peak voltage is 25 kV and the overall power consumption is about 200 W. Two configurations of the plasma actuators are shown in Fig. 4. As against to the oncoming free stream, one pair of the exposed and insulated electrodes induce velocity in the upstream direction, and the other pair induces velocity in the downstream direction, referred to as the upstream-directed actuators and the downstream-directed actuators, respectively. The exposed electrodes for both configurations of the plasma actuators are placed at $\theta = \pm 80^{\circ}$. Electrodes at higher angles may be more effective for flow manipulation. Nevertheless, there is a risk of an electric breakdown between the exposed electrodes and the metal junctions of the torque link if the two parts are too close.

It is worthwhile to mention that a jet normal to the cylinder surface can be produced if both the upstream- and downstream-directed actuators are combined together and activated simultaneously. However, little noise control performance was found in our previous experiments. An unsteady mode, where the plasma actuators are activated intermittently, was also tested in this study but with quite limited performance as well. The following discussion is therefore limited to the upstream-directed and downstream-directed actuators working at a steady mode, which continuously activates the plasma actuators with a high voltage sinusoid waveform. The frequency of the sinusoid waveform depends on the impedance of plasma actuators. For this bluff body testing case the frequency is 15 kHz after careful tuning the plasma system.

In this work the noise control effectiveness by the plasma actuators is mainly examined in an anechoic chamber facility. A nozzle (500 mm $\times$ 350 mm) connecting to a plenum chamber can produce a jet flow at speed (U_{∞}) of 30 m/s. The corresponding Reynolds numbers based on the cylinder diameter D are 2.1×10^5.

Fig. 5 shows the setup of the experimental units. The time-mean flow is visualized using particle imaging velocimetry (PIV) in the X–Z plane at approximately Y=0. The PIV system used in the experiments is produced by Dantec Measurement Systems and incorporates two Gemini Nd:YAG lasers by NewWave Research that are capable of running at 16 Hz double-pulse repetition rate, emitting pulses at 532 nm light frequency to illuminate seeding particles, which are provided to represent the flow using a Safex S195G smoke seeder by Marin Professional. The typical sizes of the non-spherical particles are 2 μm in diameter. The particles provide suitable tracer material that is homogeneously distributed into the flow. A Dantec HiSense (type 13 gain 4) 1024 $\times$ 1289 resolution charge-coupled device camera is operated in a double frame mode (2 Hz). For each experiment, 250 images of the flow field are taken for the post-processing, in which the velocity is calculated by performing time-domain analysis (cross-correlation technique) on the successive images.

Fig. 5 clearly shows that it is impossible for the present PIV system to capture the wake flow behind the cylinder, due to the obstruction of the torque link. Fig. 6 shows the other experimental configuration with the absence of the torque link. The cylinder wake flow can be studied for this configuration by the PIV system. The related flow field is certainly different from the configuration with the torque link. This study, however, is still helpful for the understanding of the flow control effects by the upstream- and downstream-directed plasma actuators.

Fig. 7 shows the overall model in the test section. It can be seen that two endplates are used to hold the bluff body model. All electric cables are outside of the test section. A microphone array is placed underneath the model to locate the

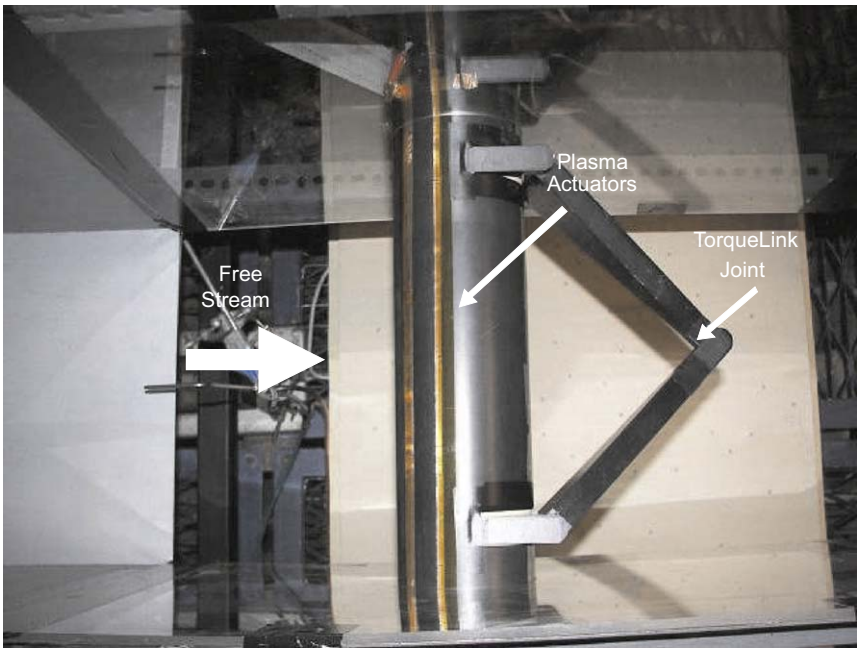

Fig. 7. The bluff body model in the test section with two endplates (top view).

near-field noise sources. The array has 56 microphones (Panasonic WM-60A). The frequency response of each microphone is calibrated to a B&K 4189 microphone. The conventional beamforming technique with shear layer correction [21] is adopted in this work for its robust performance in producing the acoustic images of sound pressure. The diameter of the array D_A is 0.64 m.

In addition, an arc containing eight instrument microphones (ECM8000 from Behringer) located at 20D away from the model is used to study the far-field sound effects (see Fig. 5). This distance is limited by the size of the anechoic chamber room. The elevation angle ϕ of each microphone is from 20° to 70°. All instrument microphones have quite good linear frequency response and omnidirectional polar pattern that help to ensure the quality of the measurements. The output from these eight microphones is passed through preamplifiers and anti-aliasing filters and subsequently is sampled with a data acquisition system produced by National Instruments at 48 kHz. A 4096 point fast Fourier transform with a Hanning window function is applied to the sampled data. The spectral results are averaged over 100 signal blocks for statistical confidence.

4. Results

Fig. 8 shows the mean velocity map of the single cylinder case in the X–Z plane. Compared to the flow field without the plasma actuation (Fig. 8(a)), the downstream-directed forcing actuation reduces the width of the wake (Fig. 8(b)), whereas the upstream-directed forcing actuation increases it (Fig. 8(c)). This finding is similar to previous experiments performed at

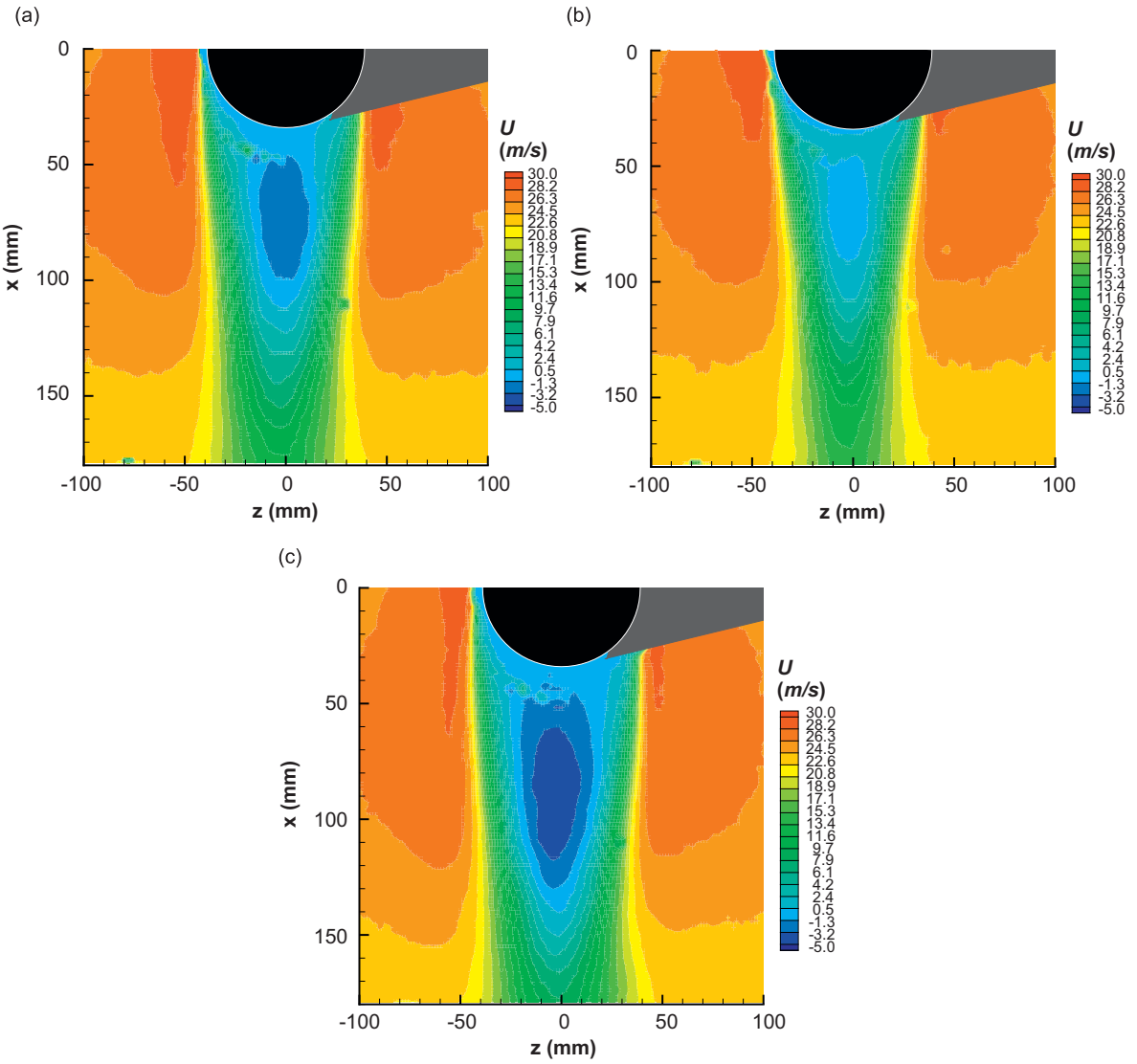

Fig. 8. Mean velocity U in the X direction, with (a) no plasma actuation, (b) the downstream-directed actuation and (c) the upstream-directed actuation.

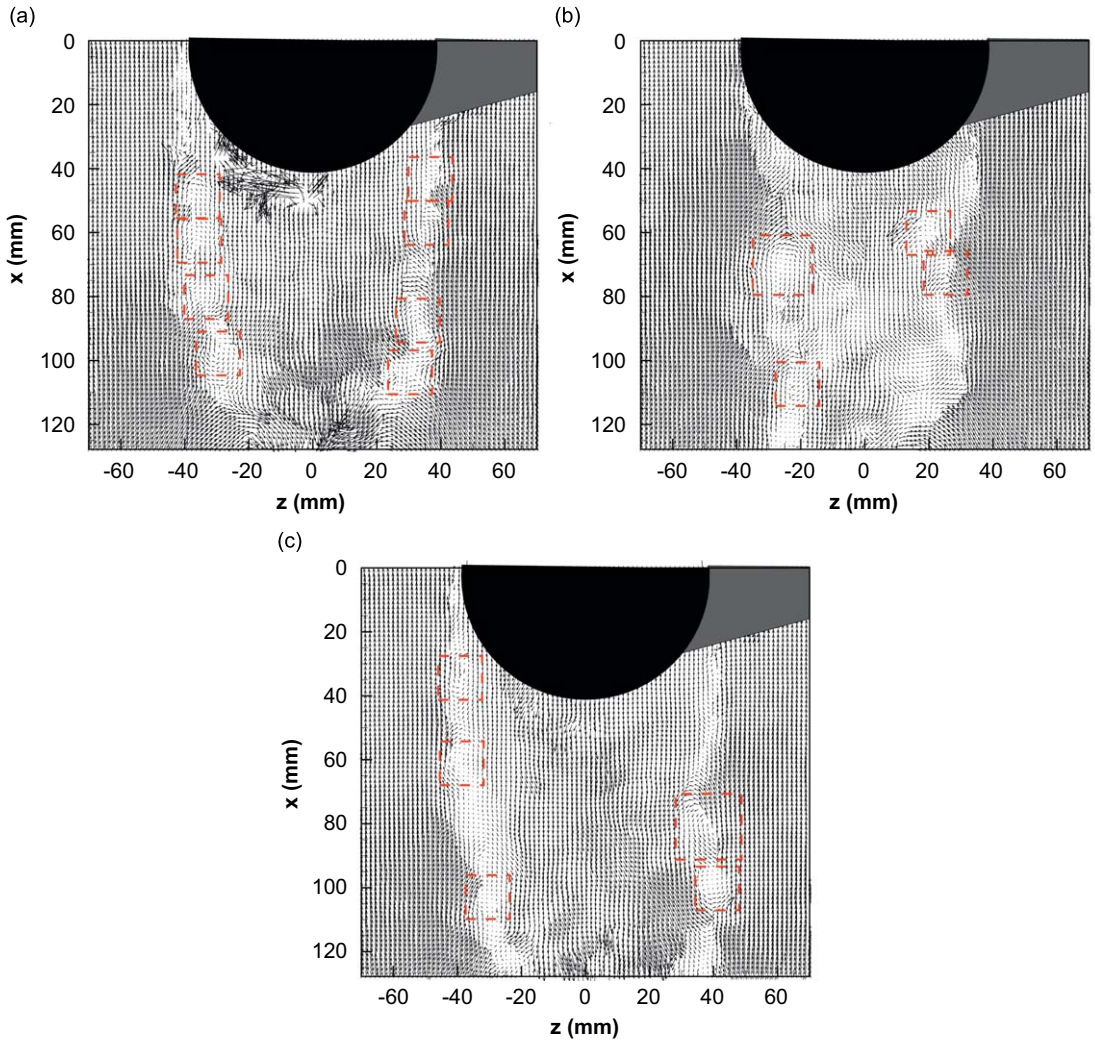

Fig. 9. Vortical structures in the cylinder wake, with (a) no plasma actuation, (b) the downstream-directed actuation and (c) the upstream-directed actuation.

lower Reynolds numbers [16,17]. Broadband noise reduction could be achieved by controlling the large scale flow structures that could alter the fine scale coherent structures further.

Vortical structures have been visualized by performing Galiean decomposition on the instantaneous velocity vectors [22]. One of the instantaneous results is shown in Fig. 9, where the vortical structures are highlighted in boxes. It can be seen that the plasma actuation, either in the upstream- or the downstream-direction, has minor effects on the length scales of the vortical structures. On the other hand, approximately 50 percent of vortical structures are absent under plasma actuations. The downstream-directed plasma actuation eliminates more vortical structures than the upstream-directed plasma actuation.

It is worthwhile to mention that the installation of a component (e.g. a torque link for this case) downstream to the cylinder should modify the cylinder wake and consequently affects the exact interference between the cylinder wake and the component. However, it is still impossible for our group to visualize the flow field details after the installation of the torque link using the present two-dimensional PIV system. The corresponding flow control effect under the upstream- or downstream-directed actuation has to be envisioned in this paper based on surface measurements and physical intuition.

The pressure fluctuations on the surface of the torque link have been measured by a surface mounted microphone (see Fig. 3). Fig. 11 shows the spectral results. The results are used to study the interference between the cylinder wake and the downstream component. The main attention is focused on the results at low frequency ranges that represent most energetic dynamics of the large scale flow structures. It can be seen that the pressure fluctuations at the frequency range below 130 Hz is reduced by 3.7 ± 0.8 dB with the upstream-directed actuation, which suggests that an upstream-directed plasma actuator could reduce the wake impinging on the torque link surface extensively. In contrast the pressure fluctuation is just affected a little at the same low frequency ranges with the downstream-directed plasma actuation.

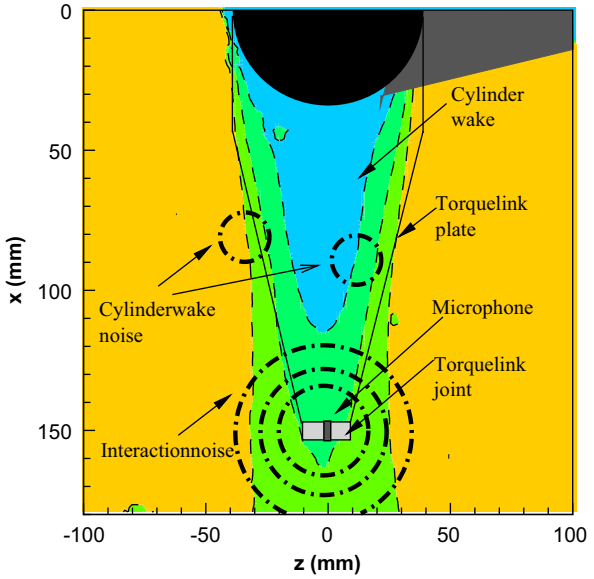

Fig. 10. Potential noise source in the flow (top view).

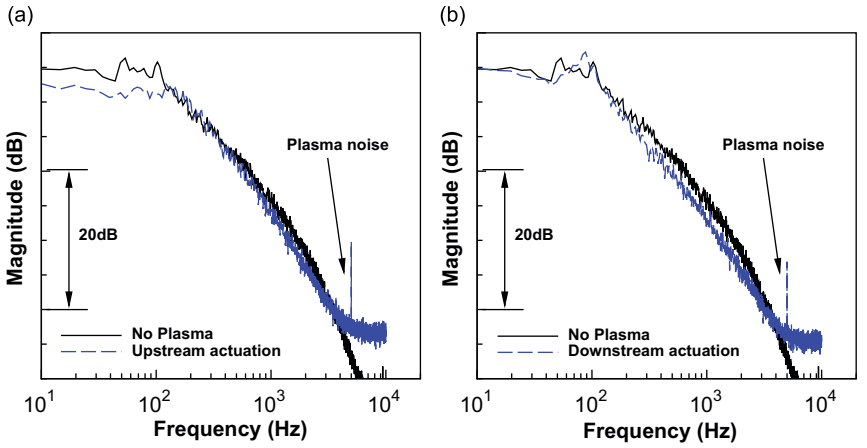

Fig. 11. The spectral of the surface pressure fluctuation on the torque link, where (a) the upstream-directed plasma actuators are activated and (b) the downstream-directed plasma actuators are activated. $U_\infty = 30\,\mathrm{m/s}$.

On the other hand, at the frequency ranges between 400 Hz and 3 kHz, the spectral reduction is 1.3 ± 0.6 dB by the upstream-directed plasma actuation, and 3.6 ± 0.6 dB by the downstream-directed plasma actuation. In addition, as the hand-made antialiasing filter is a simple and cheap first-order passive filter, its filtering performance at high frequency beyond 3.5 kHz is incompetent. For example, a peak at 5 kHz is actually the ghost image of the plasma tonal noise at 15 Hz, bear in mind that the Nyquist frequency for this sampling is 10 kHz.

Fig. 10 analysis the potential flow-induced sound sources for the case, which include the sound from the cylinder wake itself and the sound generated due to the wake impingement on the torque link surface. The spectral changes in Fig. 11 could suggest that both the upstream- and the downstream-directed plasma actuators could be effective in noise attenuation applications. The spectral results are measured at the center of the downstream torque link (see Fig. 3) and could represent pressure oscillations over the whole surface. It appears that the upstream-directed plasma actuation acts as a virtual fairing that could reduce the flow speed impinging on the surface of the torque link extensively. The downstream-directed plasma actuations have few effects in controlling the impingement whereas could eliminate more vortical structures (see Fig. 9). As a result, more reduction in surface pressure spectra can be found at high frequency ranges with the downstream-directed plasma actuations.

Furthermore, acoustic measurements have been conducted to investigate the specific noise control performance. Microphone array and beamforming signal processing [23] have been increasingly used to investigate acoustic source changes. Figs. 12 and 13 show the acoustic images results at 5 and 3.5 kHz in dB, respectively. The beamforming resolution at a frequency lower than 1 kHz is, however, unacceptable and not shown here [21]. In addition, the sound pressure levels

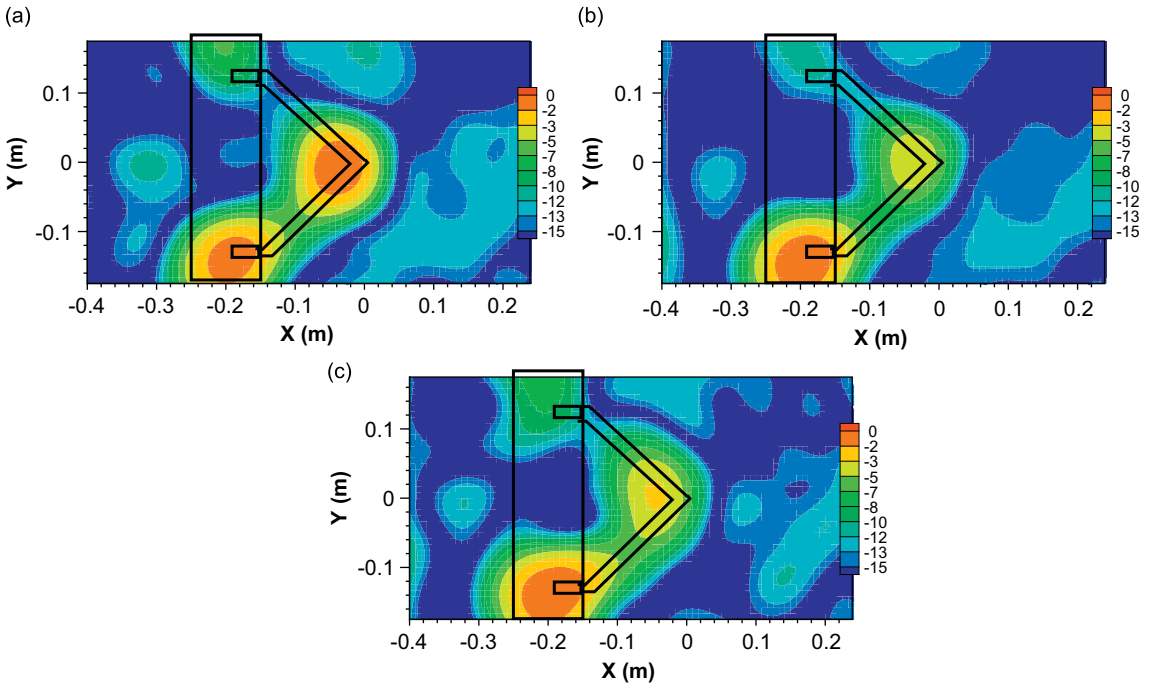

Fig. 12. Acoustic images of SPL in dB at f=5 kHz, $U_\infty = 30$ m/s, Z=0, adopting (a) inactive actuation; (b) the upstream-directed actuation; and (c) the downstream-directed actuation.

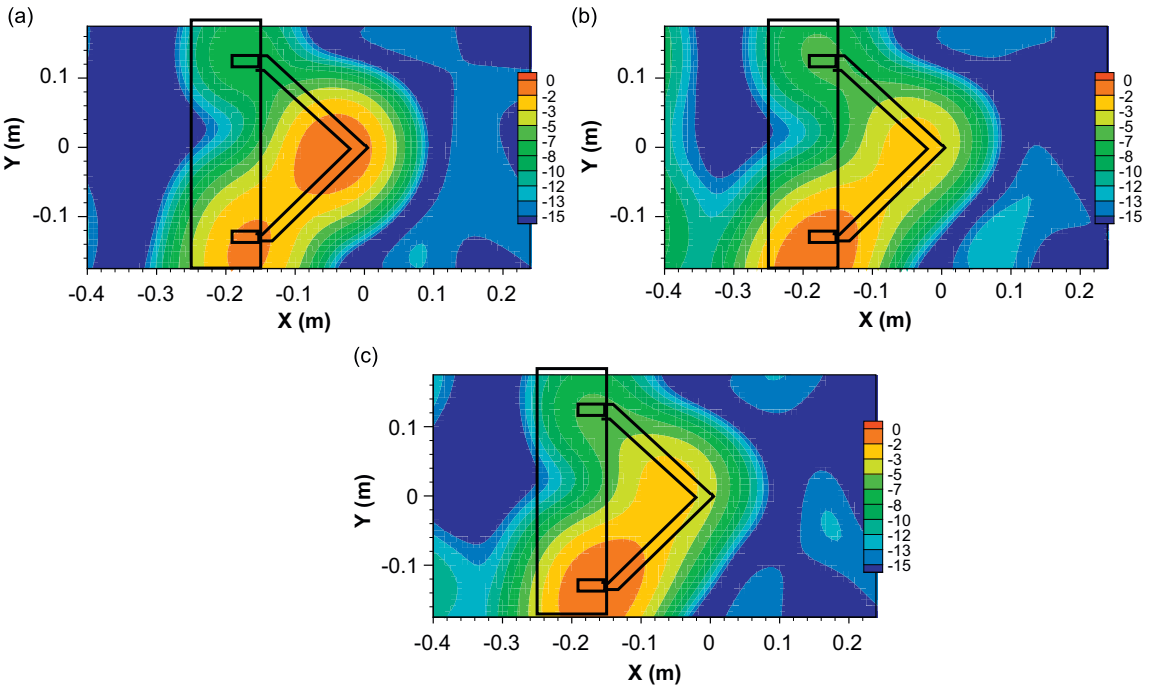

Fig. 13. Acoustic images of SPL in dB at f=3.5 kHz, $U_\infty = 30$ m/s, Z=0, adopting (a) inactive actuation; (b) the upstream-directed actuation; and (c) the downstream-directed actuation.

(SPL) for these figures have been nondimensionalized by the maximal SPL value measured without any actuation. It can be seen that the SPL of the dominant source around the torque link joint is reduced by up to 3.5 ± 0.3 dB at 30 m/s, and the performance of the upstream-directed actuators is better than that of the downstream-directed actuators. Similar findings are also found at other frequencies.

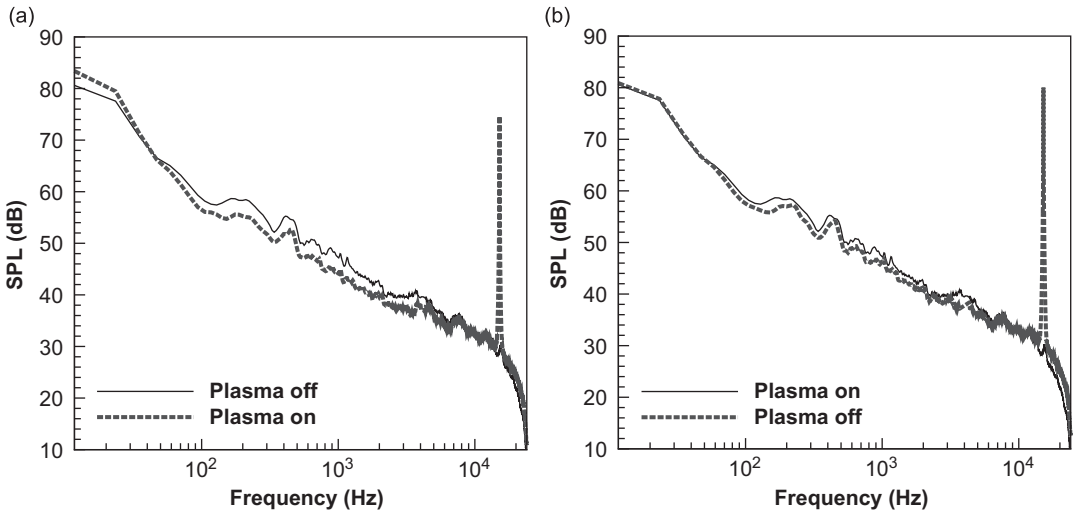

Fig. 14. Far-field SPL results with (a) the upstream-directed actuation, and (b) the downstream-directed actuation. $U_\infty = 30\,\mathrm{m/s}$.

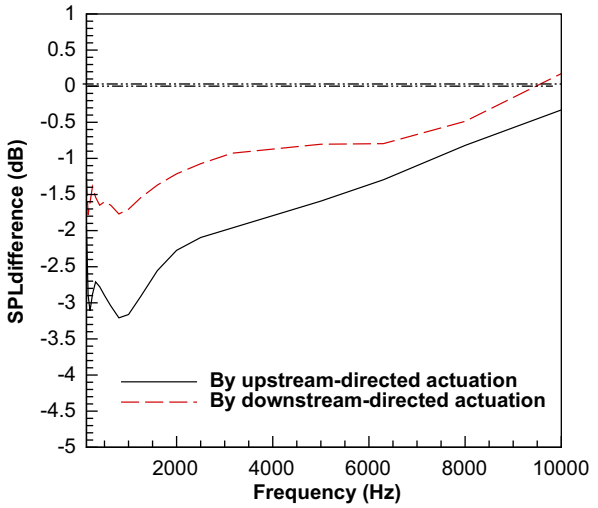

Fig. 15. The SPL difference on the $\frac{1}{3}$ octave band. $U_\infty = 30\,\mathrm{m/s}$.

It can be found that the correlation between the on-surface pressure history and the off-surface acoustic measurements is limited, possibly due to the nonlinear aeroacoustic physics [24]. For example, Fig. 12 suggests that the acoustic strength can be reduced by the plasma actuation at 5 kHz. The similar findings cannot be found in Fig. 11.

Fig. 14 compares the far-field SPL results of the top microphone over broadband frequencies at $U_\infty = 30\,\mathrm{m/s}$. The results from all other seven microphones are similar and therefore not shown here for brevity. A tonal noise that can be found in previous cylinder experiments [16] at the shedding frequency (approximately 63 Hz) is absent for our case. This tonal noise could be overwhelmed by the background noise from the high pressure chamber. The installation of the torque link also could prevent the shedding from appearing at a certain frequency. The exact reason of the absence of a tonal noise at the shedding frequency is still unknown.

In addition, it can be seen that the upstream-directed actuation attenuated noise more effectively, especially at the frequency ranges from 1 to 3 kHz. There is up to 3 ± 0.2 dB reduction with the upstream-directed actuation; whilst up to 1.7 ± 0.2 dB reduction with the downstream-directed actuation. The noise control effect is diminished at higher frequencies due to the interference from the self-noise of the plasma actuators, which is especially dominant at the working frequency f_p=15 kHz. The problem can be resolved later by increasing the f_p beyond 20 kHz.

The noise control performance by two types of plasma actuators are compared on the $\frac{1}{3}$ octave band in Fig. 15, where a negative value denotes the noise reduction due to the plasma actuation. Fig. 15 clearly shows that for this case the upstream-directed plasma actuators perform better than the downstream-directed plasma actuators. It can be seen that the upstream-directed plasma actuation can reduce sound level by up to 3.2 dB from 1 to 3 kHz. The noise control effect is

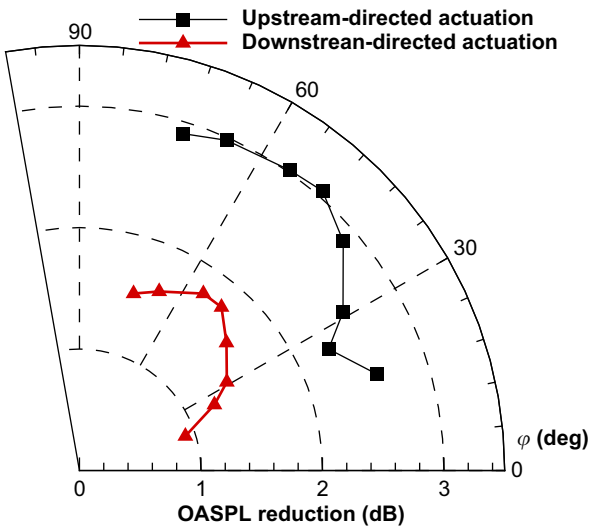

Fig. 16. The OASPL reduction values measured by the microphones on the arc. $U_\infty = 30\,\mathrm{m/s}$.

reduced along with the increase of the frequency. The sound level is even increased beyond 10 kHz that is caused by the self-noise radiating from plasma actuators.

The absolute reductions in terms of the overall sound pressure level (OASPL) with respect to different measurement angles (ϕ) are shown in Fig. 16. The frequency band used for the computation of OASPL is from 125 Hz to 8 kHz. It is clear that the upstream-directed plasma actuators worked more efficiently for noise control. The OASPL reduction with it are up to approximately 3 dB at most radiation angles. The corresponding OASPL reductions with the downstream-directed actuation are up to 1.7 dB only.

5. Summary

The aim of this experimental investigation was to study the control effectiveness of the plasma actuators on broadband noise radiated from a bluff body. Acoustic measurements using a near-field microphone array and a far-field microphone arc were conducted at 30 m/s. Either the upstream-directed actuation or the downstream-directed actuation was applied on the cylinder surface. Flow measurements using PIV suggested that the cylinder wake could be manipulated with either plasma actuation. Acoustic measurements also showed that the strength of the dominant noise source was reduced. It can be found that the noise control effect with the upstream-directed actuation is better than that of the downstream-directed actuation. Similar findings have been discovered in our lab for bluff body models with various configurations, such as a cylinder with a flat plate, etc., that proves the generic capability and benefit of the flow control strategy with the upstream-directed actuation. It was also found in our experiments at higher speeds ($U_\infty = 40-50\,\mathrm{m/s}$) that the noise control performance of the plasma actuators deteriorated. To further reduce broadband noise, additional reduction of the interaction between the cylinder wake and the torque link component could be achieved by improving the plasma actuator performance. Improved power supply with higher AC voltage and/or alternative plasma actuators, such as DC corona plasma actuators, could be considered next.

Acknowledgments

This work was mainly supported by TIMPAN (Technology to IMProve Airframe Noise) project, which is co-funded by the European Commission and the sixth Framework Programme (2002–2006). We would like to acknowledge Dr. L.C. Chow of Airbus for helpful discussions throughout the work. During the preparation of this paper, the corresponding author was supported by the NSF Grant of China (Grant 90916003).

References

[1] J.R. Roth, D.M. Sherman, S.P. Wilkinson, Electrohydrodynamic flow control with a glow-discharge surface plasma, *AIAA Journal* 38 (7) (2000) 1166–1172.
[2] H.H. Brouwer, S.W. Rienstra, Aeroacoustics research in Europe: the CEAS-ASC report on 2007 highlights, *Journal of Sound and Vibration* 318 (4–5) (2008) 625–654.
[3] S. Chan, X. Zhang, S. Gabriel, The attenuation of cavity tones using plasma actuators, *AIAA Journal* 45 (7) (2007) 1525–1538.

[4] X. Huang, S. Chan, X. Zhang, An atmospheric plasma actuator for aeroacoustic applications, *IEEE Transactions on Plasma Science* 35 (3) (2007) 693–695.
[5] X. Huang, S. Chan, X. Zhang, S. Gabriel, Variable structure model for flow-induced tonal noise control with plasma actuators, *AIAA Journal* 46 (1) (2008) 241–250.
[6] X. Huang, X. Zhang, Streamwise and spanwise plasma actuators for flow-induced cavity noise control, *Physics of Fluids* 20 (3) (2008) 037101(1–10).
[7] F. Massines, A. Rabehi, P. Decomps, R.B. Gadri, P. Ségur, C. Mayoux, Experimental and theoretical study of a glow discharge at atmospheric pressure controlled by dielectric barrier, *Journal of Applied Physics* 83 (6) (1998) 2950–2957.
[8] J. Ráhel, D.M. Sherman, The transition from a filamentary dielectric barrier discharge to a diffuse barrier discharge in air at atmospheric pressure, *Journal of Physics D: Applied Physics* 38 (4) (2005) 547–554.
[9] M. Samimy, J.H. Kim, J. Kastner, I. Adamovich, Y. Utkin, Active control of high-speed and high-Reynolds-number jets using plasma actuators, *Journal of Fluids Mechanics* 578 (2007) 305–330.
[10] P. Gnemmi, R. Charon, J.P. Duperoux, A. George, Feasibility study for steering a supersonic projectile by a plasma actuator, *AIAA Journal* 46 (6) (2008) 1308–1317.
[11] P.Q. Elias, B. Chanetz, S. Larigaldie, D. Packan, Study of the effect of glow discharges near a $M=3$ bow shock, *AIAA Journal* 45 (9) (2007) 2237–2245.
[12] L. Léger, E. Moreau, G.G. Touchard, Effect of a dc corona electrical discharge on the airflow along a flat plate, *IEEE Transactions on Industry Applications* 38 (6) (2002) 1478–1485.
[13] D. Greenblatt, B. Göksel, I. Rechenberg, C.Y. Schüle, D. Romann, C.O. Paschereit, Dielectric barrier discharge flow control at very low flight Reynolds numbers, *AIAA Journal* 46 (6) (2008) 1528–1541.
[14] E. Moreau, Airflow control by non-thermal plasma actuators, *Journal of Physics D: Applied Physics* 40 (2007) 605–636.
[15] J.R. Roth, D.M. Sherman, S.P. Wilkinson, Boundary layer flow control with a one atmosphere uniform glow discharge surface plasma, *AIAA Paper* 1998–0328, 1998.
[16] O.F. Thomas, A. Kozlov, C.T. Corke, Plasma actuators for landing gear noise reduction, *AIAA Journal* 46 (8) (2008) 1921–1931.
[17] Y. Sung, W. Kim, M.G. Mungal, M.A. Cappelli, Aerodynamic modification of flow over bluff objects by plasma actuation, *Experiments in Fluids* 41 (2006) 479–486.
[18] M. Forte, J. Jolibois, J. Pons, E. Moreau, G. Touchard, M. Cazalens, Optimization of a dielectric barrier discharge actuator by stationary and non-stationary measurements of the induced flow velocity: application to airflow control, *Experiments in Fluids* 43 (6) (2007) 917–928.
[19] E. Peers, X. Huang, X.F. Luo, A numerical model of plasma actuators effects in flow-induced noise control, *IEEE Transactions on Plasma Science* 37 (11) (2009) 2250–2256.
[20] Z.Y. Chen, Pspice simulation of one atmosphere uniform glow discharge plasma (oaugdp) reactor systems, *IEEE Transactions on Plasma Science* 31 (4) (2003) 1–10.
[21] T.J.E. Mueller, *Aeroacoustic Measurements*, Springer, Germany, 2002.
[22] R.J. Adrian, K.T. Christensen, Z.C. Liu, Analysis and interpretation of instantaneous turbulent velocity fields, *Experiments in Fluids* 29 (3) (2000) 275–290.
[23] X. Huang, Real-time algorithm for acoustic imaging with a microphone array, *Journal of Acoustical Society of America Express Letters* 125 (5) (2009) EL190–EL195.
[24] J.E. Ffowcs-Williams, D.L. Hawkings, Sound generation by turbulence and surfaces in arbitrary motion, *Philosophical Transactions of the Royal Society of London A* 264 (1969) 321–342.